The HANDS-IONS Daytime Camera for GEO Satellite Characterization

Kevin T.C. Jim, Randy Wolfshagen, Brooke Gibson, Edward A. Pier
Oceanit, Oceanit Center, 828 Fort St. Mall #600, Honolulu, HI 96813

Klaus W. Hodapp
Institute for Astronomy, University of Hawaii, 640 North A`ohoku Place #209, Hilo, Hawaii 96720

Peter Onaka
Institute for Astronomy, University of Hawaii, 2680 Woodlawn Drive, Honolulu, Hawaii 96822

Daytime imaging of GEO satellites is challenging due to the bright background of the daytime sky. However, with the appropriate selection of wavelengths, we show that it is possible to detect GEO satellites in the infrared. The design of the purpose-built camera system for detecting GEO satellites is discussed, along with the anticipated performance of the system.

1. Introduction

Daytime imaging or detection of geosynchronous earth-orbiting (GEO) satellites in visible or infrared (IR) wavelengths has not been reported in the literature, although low Earth-orbiting (LEO) objects have been observed routinely [1]. Yet detecting such satellites in optical or IR wavelengths is desirable because the alternative ground-based method, radar, is expensive to deploy and operate. Daytime optical/IR detection would have significant SSA applications. In addition, there is significant work in development to characterize the attitude, shape, and size of satellites using photometric light curves [2]; obtaining light curves in many phase angles can improve the ASR solutions [3]. In order to determine the feasibility of such imaging, we engaged in a series of simulations, whose theoretical basis is described previously [4]. Further simulations have shown that daytime observations are possible with a slightly modified, astronomical camera design. We also engaged in a test observation in which stars of brightness comparable to the GEO satellites were imaged during the daytime with the NASA Infrared Telescope Facility (IRTF), which will be described in the future [5].

In our simulations, done for Haleakala, we considered the summer solstice and looked at the sky radiance and transmittance as a function of look angle and time of day, as described in our companion paper in this conference [6]. The look angles were spaced 10° along the mean geosynchronous belt. Using MODTRAN and actual weather data, including radiosonde data, to simulate the sky radiometry, and combining this with a full simulation of telescope optics and sensor noise sources, we found that the optimal filter for observations were either the *K-short* or *K* filters. We assumed an empirically derived albedo, which is much like a diffuse sphere. A plot of the dependence of the SNR on look angle and time is shown in Fig. 1. Shorter wavelengths have lower SNRs due to the much higher background from the blue daytime sky. At longer wavelengths, the rapid decrease in the solar spectrum reduces the flux reflected from satellites. This is discussed more fully in [6].

In actual operation, the camera is designed to be used for both daytime and nighttime observing. At night, with a much lower sky background, the camera will operate exactly like a standard astronomical IR camera.

2. Site Considerations

We evaluated a series of sites that might be most suitable for daytime imaging of GEO satellites. Our criteria were:

- High altitude (greater than 2 km) to get above much of the water vapor in the atmosphere
- Moderate latitude (less than 40° N latitude) to be able to observe the GEO belt without high airmass
- Existing observatories with telescopes primary mirrors 1-m or greater
- In the western continental USA or Hawaii, to simplify logistics for our Hawaii-based operations
- Observatories willing to work with our unusual observing regime, and with reasonable deployment costs for our Hawaii-based development

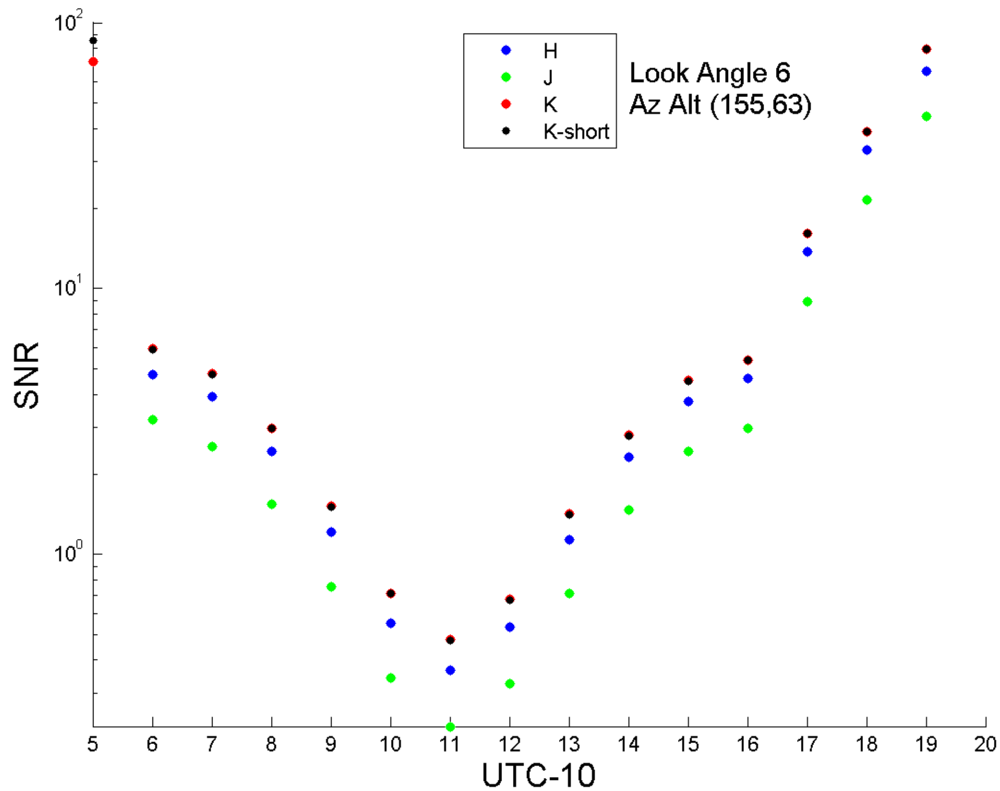

Figure 1: The SNR vs. time looking to the South-East into the GEO belt from Haleakala during the daytime. The dip in the SNR occurs where the Sun is close to the observed position. This simulation assumes a 2.2-m primary size, with a satellite diameter of 5-m, with a diffuse reflectance, operating the MANTIS imager in the 70 Ke- full well mode with CDS and 1-s exposures.

The observatories that satisfy our final selection criteria are tabulated below in Table 1. The camera has been designed to be able to operate at these telescopes, but it is also possible to modify the camera to operate with other telescopes. To move the camera from one telescope to another requires changing the mounting adapter on the front of the camera and rotating the filter wheel so that the appropriate Lyot stop is in the beam. In addition, the external cooling compressor, which is not a part of the camera, must be connected.

As can be seen from Table 1, the most stringent physical requirements come from the University of Utah W.L. Eccles Observatory, which was slightly smaller than our desired 1-m aperture. However, the flexibility and cooperation of the operators of this telescope, and the excellent site, pushed it onto our list. The camera, designed to fit onto the Utah telescope, will fit into all of the other telescope instrument envelopes.

Initial operations will start with the University of Hawaii 2.2-m telescope on Mauna Kea, which is also the highest and best site for atmospheric conditions.

3. Optical Design

The optical system is a classical refractive re-imaging design with a pupil image where a cold Lyot stop will be placed. The optical layout is shown in Fig. 2. Following the optical path shown in Fig. 2, the light enters through a quartz window, where the telescope pupil is projected onto a Lyot cold stop, which is necessary to suppress the IR radiation from the telescope itself. Then, re-imaging optics and a field lens form the final image on the focal plane array. The lenses are made from barium fluoride, except for the second lens, which is made from Ohara S-NPH2 glass. The last two lenses are aspheres. All lenses are anti-reflection coated from 1.0 to 2.4 μm. The plate scale at our initial test site, the University of Hawaii 2.2-m telescope, is 0.4 "/pixel, and the field of view will be 0.14°×0.11°. The FOV and plate scales on other telescopes are described in Table 1.

Table 1: Candidate telescopes for the daytime GEO imaging system.

Telescope Name	UH 2.2m	AMOS 1.6 m	Mt. Lemmon	Willard L. Eccles Observatory
Location	Mauna Kea, HI	Haleakala, HI	Catalina Mountains NE of Tucson, AZ	Frisco Peak, UT
Operator	University of Hawaii	AFRL	University of Minnesota	University of Utah
Latitude [°]	19.83 N	20.71 N	32.44 N	38.52 N
Longitude [°]	155.47 W	156.26 W	110.79 W	113.28 W
Elevation [m]	4205	3058	2776	2991
Daytime seeing estimate, K ["]	1.2	1.6	3	3
Aperture [m]	2.2	1.6	1.52	0.8
Telescope native f/#	f/10	f/16	f/14.5	f/8
Camera Mounting point	bent-Cassegrain	Blanchard	Cassegrain	Cassegrain
Camera Field of view ["]	512 × 410	448 × 358	512 × 410	1766 × 1413
Camera Field of view [°]	0.14 × 0.11	0.12 × 0.10	0.14 × 0.11	0.49 × 0.39
Camera Platescale [arcsec/pixel]	0.4	0.35	0.4	1.38
Allowed instrument mass	90.7kg +	90.7kg +	90.7kg +	90.7 kg
Instrument envelope	Large	Large	Large	0.81 m from mount to fork
URL	http//www.ifa.hawaii.edu/88inch/	http//www.maui.afmc.af.mil/	http//ir.astro.umn.edu/telescopes/mlof.html	http//www.physics.utah.edu/weo/weo_techspecs.html

The camera is designed to be mounted at the Cassegrain focus of one of the candidate telescopes. The camera is cryogenically cooled using a two-stage, closed cycle, helium-based cooler. The optical system will be cooled by the first stage of the cryocooler to about 100K.

At the re-imaged pupil, there are two filter wheels. Each wheel can hold 5 one-inch round optical elements and is coupled to the first stage of the cryocooler. The first wheel will hold a blank that will be used to gather dark calibration images. It will also hold the Lyot stops sized for different telescopes. The second wheel will hold the Mauna Kea *J, H, K*, and *K-short* filters[7].

To perform experiments to reduce the background caused by polarized light, a warm, rotating 1/2-wave plate is located in front of the dewar window. The ½-wave plate can be moved in and out of the beam remotely. A wire grid combined with the Lyot stop is then put into the first rotating filter wheel.

On the University of Hawaii 2.2-m Telescope, the camera will be mounted on one of the two bent-Cassegrain positions, which can be rapidly switched between normal Cassegrain and the other bent-Cassegrain positions.

Our expectation is that the system optics will have excellent throughput. The camera optical throughput is better than 0.79, the optical throughput of the telescope is better than 0.80, and the total optical throughput is better than 0.64 without the filters. The FPA quantum efficiency should be better than 0.85.

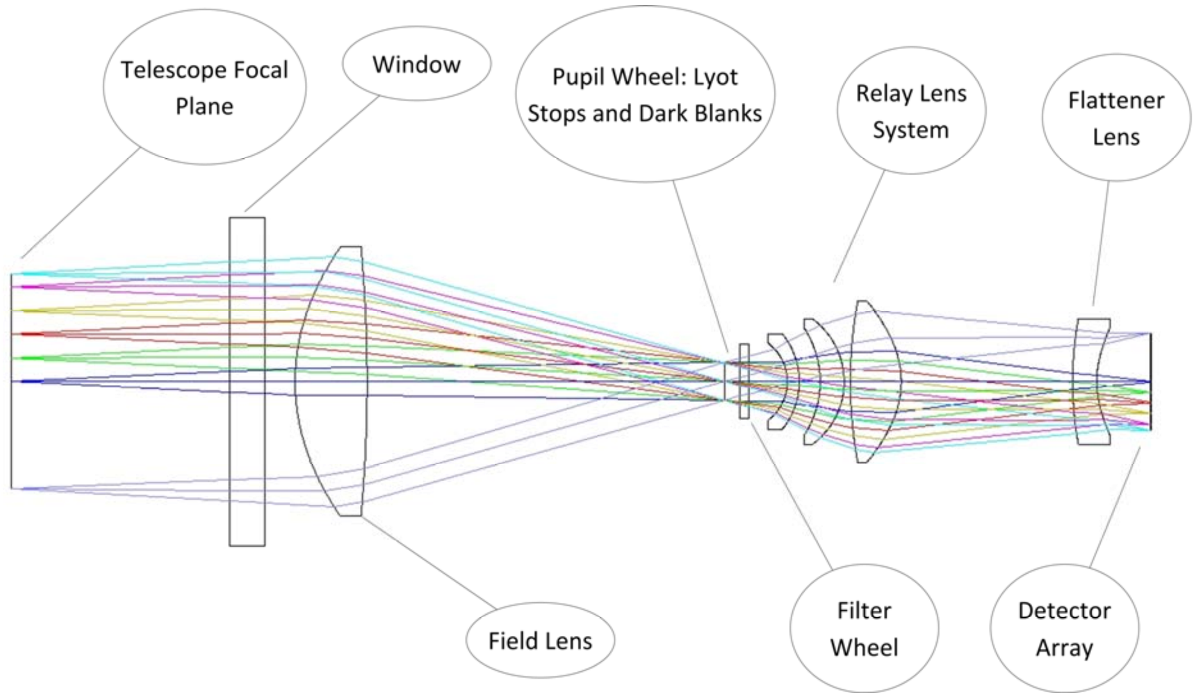

Figure 2: The optical layout of the HANDS-IONS camera.

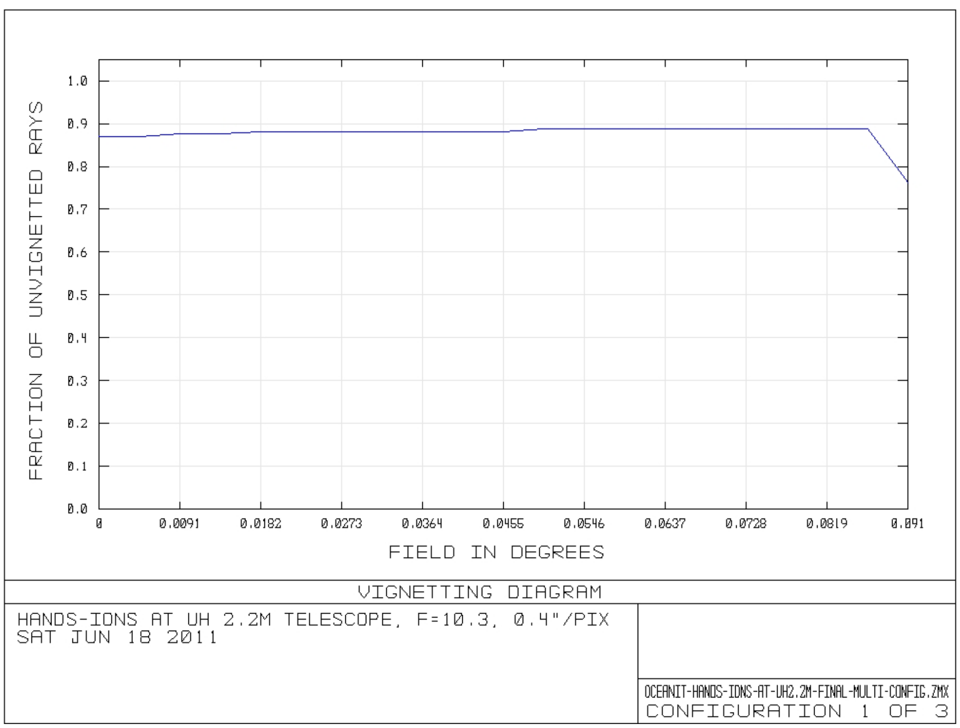

Figure 3: Vignetting of the field only occurs at the very edges, and a 1000 x 1000 pixel region is unvignetted. Even at the edge of the field the amount of vignetting is perfectly acceptable for imaging.

4. System Design

The HANDS-IONS system includes the camera and computers to operate the camera and analyze the data. The camera itself has a series of functional components, which are supported by either microcontrollers or directly connected to a data reduction Ethernet (see Fig. 8). A CTI Cryogenics Cryodyne Refrigerator Model 22 two-stage, closed cycle, Helium refrigeration system is used to cool the focal plane (80K) and optics (100K) with an external compressor attached via gas lines. The compressor is located one floor below the telescope, to vent heat outside of the dome and to decouple vibrations.

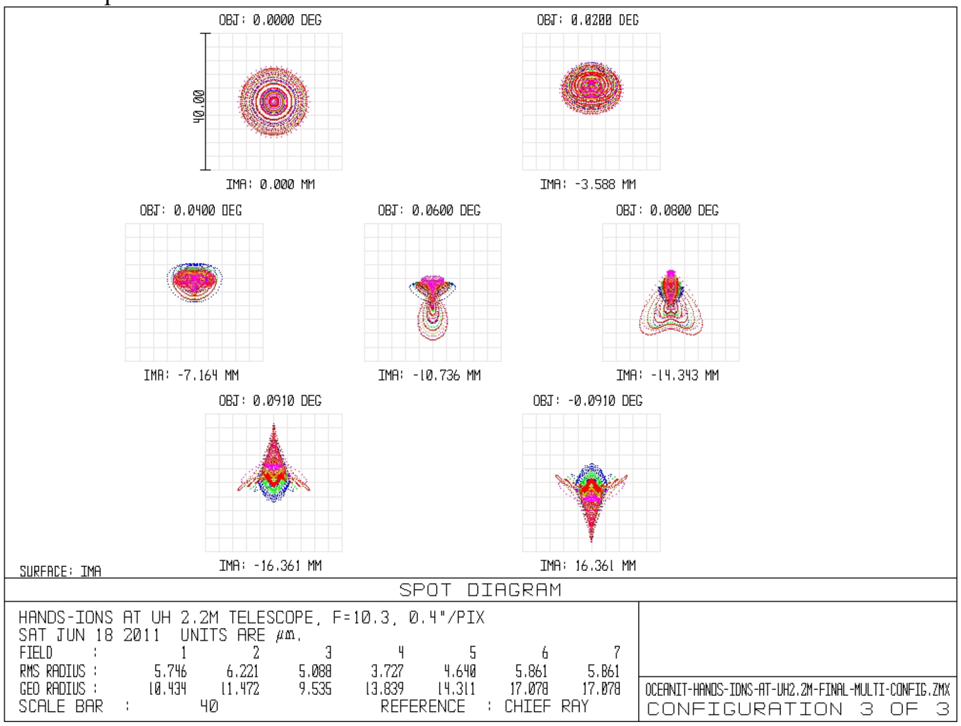

Figure 4: Spot diagram for J filter on the UH telescope. The pixels are 20 µm square, with a plate scale of 0.4"/pixel. The expected daytime seeing is 1" or worse; 1.2" has been observed.

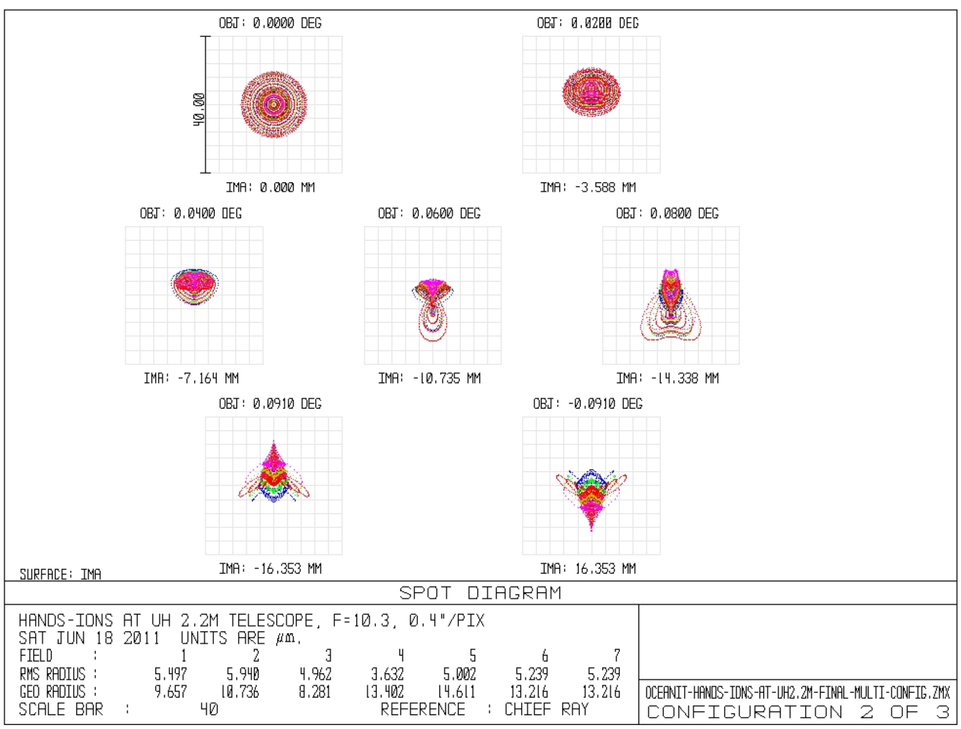

Figure 5: Spot diagram for H filter on the UH telescope.

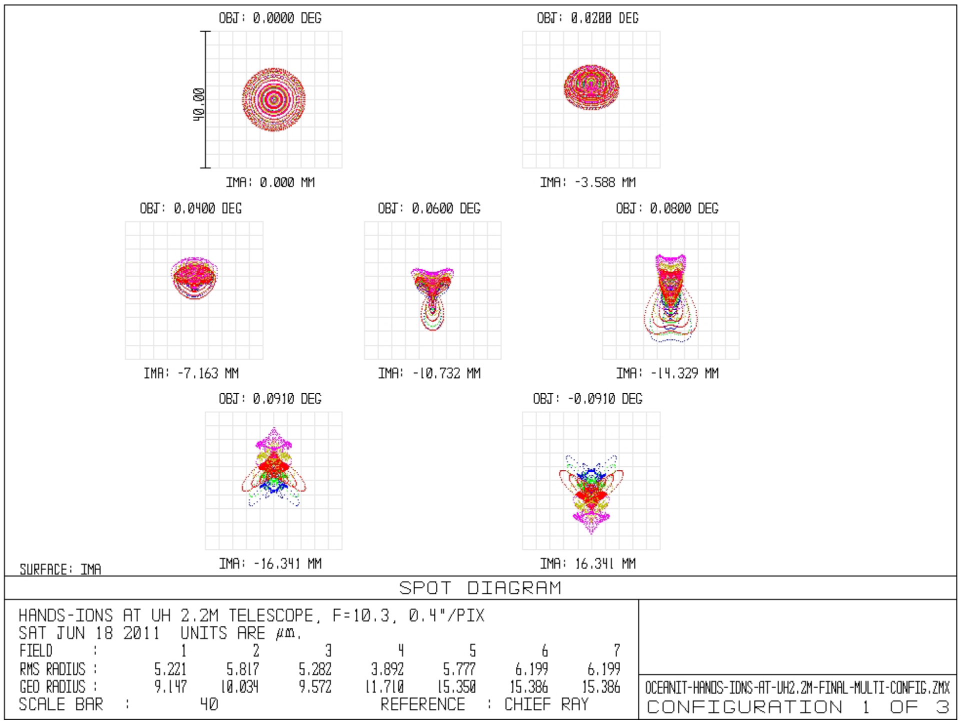

Figure 6: Spot diagram for the K filter.

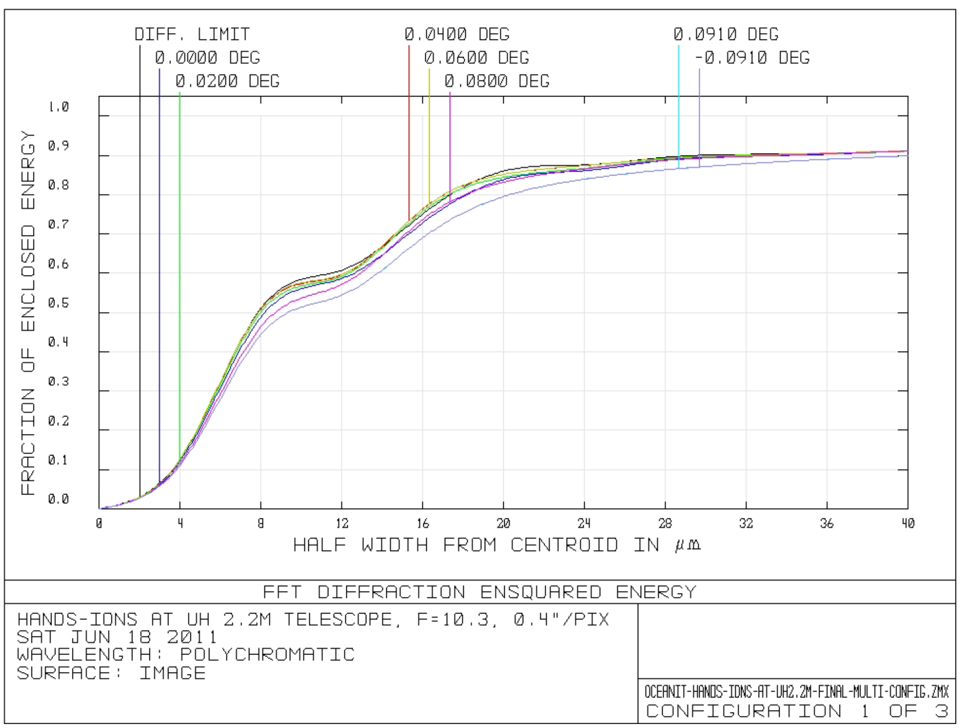

Figure 7: En-squared energy in the K filter. 90% of the energy falls within a two-pixel width, which is less than the expected seeing.

5. Focal Plane Array

The focal plane array (FPA) selection was driven by our experience at the IRTF with a successful observation with a low-noise astronomical camera system (SpEX) and our simulations showing background sky brightness in the range of 6 mag/sq. arcsecond. For the FOV we were considering, that meant that photon count per pixel would be between 250 Ke-/s to 700 Ke-/s. This drove us toward a faster sensor or one with a larger full well, but with low read noise. Imaging will always be background-limited.

Our choice is the SB-339 1280 x 1024 CTIA design, which was funded by DARPA on the MANTIS (Multispectral Adaptive Networked Tactical Imaging System) project in 2003. The MANTIS SCA (Sensor Chip Assembly) is based on a HgCdTe 80 K SWIR detector FPA (Focal Plane Array) design, mated to the RVS SB-339 ROIC (Read-out Integrated Circuit)[8]. The SCA was designed for SWIR with flat QE of 85% from 0.9 to 2.5µm, with 20 µm square pixels in a 1280×1024 format. Other formats are also available, including 640×512, 1920×512 pixels, as well as FPA's with SWIR InGaAs and LWIR HgCd Te detector materials.

The SB339 ROIC supports variable integration times for two gain settings with two different full wells, allowing coverage over a very wide range of backgrounds. The high gain (26uV/e-) mode is Capacitive Feedback Transimpedance Amplifier (CTIA)-based with an input referred noise (25 e- to 30 e- read noise with Correlated Double Sampling (CDS)) that is resistant to pickup noise [8,9]. The high gain mode has a 70 Ke- full well, a snapshot shutter, and non-destructive read. The high read rates (up to 60 Hz) allow working at high backgrounds. The current design of the electronics will limit the frame read rate to 20Hz, but that will still allow for CDS sampling at 700K e-/sec background. The low gain (0.42uv/e-) mode uses a Source Follower per Detector (SFD) amplifier with a large well capacity of at least 2.2 Me-; in this mode, the device uses a rolling shutter and destructive read. We plan to experiment with both modes to determine the range of sky backgrounds through which satellites can be observed. It may also be possible to sum images in the camera controller, reducing the bandwidth.

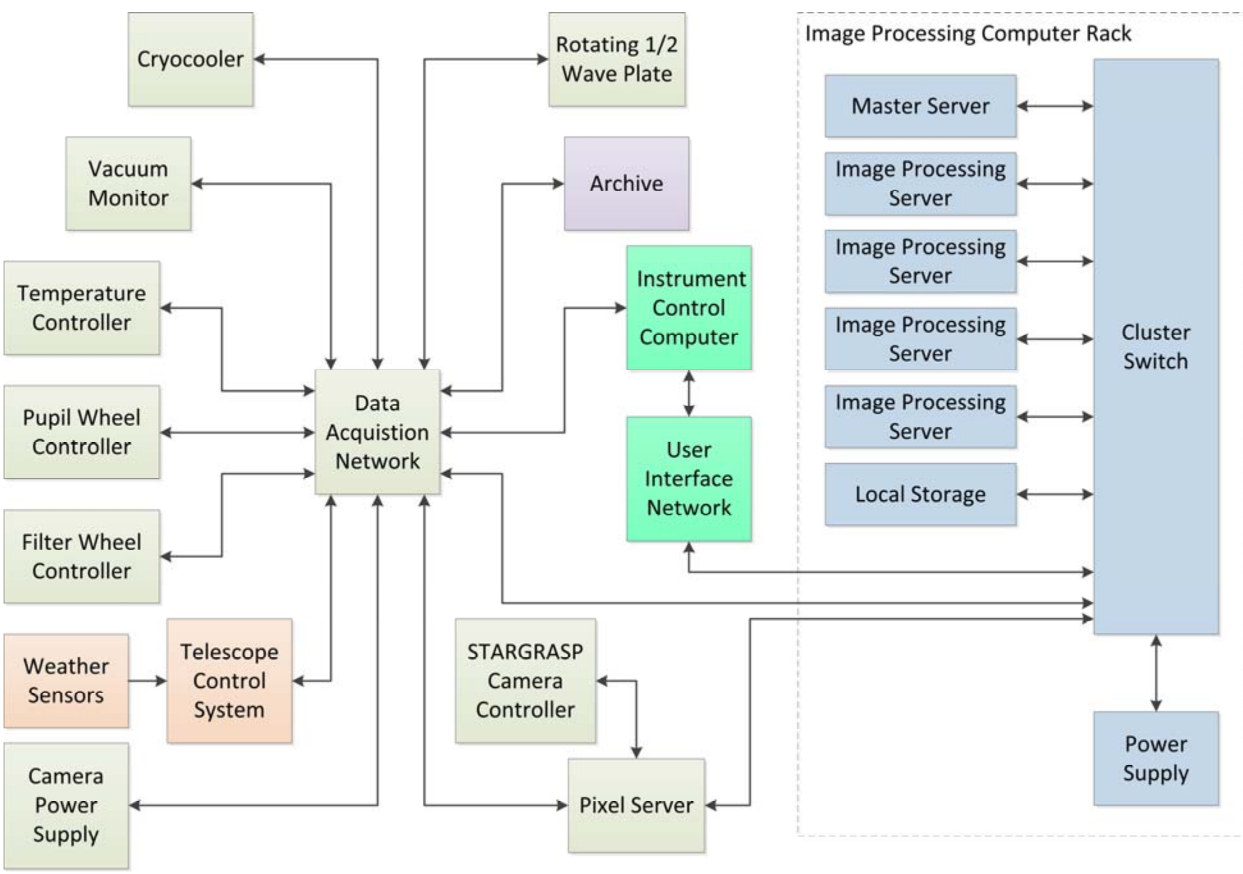

Figure 8: System layout of the camera. Communications are through Ethernet. The STARGRASP controller has a dedicated link to the data acquisition computer (the Pixel Server.)

6. Camera Controller

The HANDS-IONS camera will use the IfA-designed STARGRASP controller [10], originally designed to operate the Pan-STARRS PS-1 Gigapixel camera. The HANDS-IONS camera will use one controller board set, consisting of the DAQ3U motherboard, Xilinx FPGA daughtercard, and a pre-amp card. The motherboard has 16, three-channel, 16-bit analog to digital converters (ADC) running at 10 MHz. The daughtercard has a Xilinx Virtex2 Pro FPGA with a 300 MHz PowerPC implemented in the FPGA, 512 MB of RAM, and gigabit Ethernet. The preamp board can be AC or DC-coupled, and we will use DC-coupling for our design. The first stage of pre-amplification is an opamp, Ibias AD797 or AD829. The second stage is a Bessel filter, bandpass-tuned for optimal noise. Digital multi-sampling is used to reduce the read noise. The Gigapixel camera, as used on Haleakala, has been measured to have 7 e- of read noise [11].

The focal plane is coupled with a short, impedance-matched, Ridgid-flex cable that is epoxied through a hole through the camera head. The camera controller box is mounted directly onto the camera dewar body, maintaining a Faraday cage around the cabling.

The controller is tied to the instrument control computer via Gig-E, with a fiber optic media change to reduce possible stray RF radiation in the dome. This link is a dedicated network segment. The maximum throughput is about 24 frames per second at the 1280×1024 pixel image size of our MANTIS imager.

The Pan-STARRS software is written in C and runs under Linux on the Xilinx FPGA. It will be modified to support the Raytheon MANTIS imager.

7. Data Reduction System

We have designed a data reduction system that will reduce the data in near real-time. It is based on a parallelized version of the standard image processing algorithms for nighttime astronomical infrared imaging. In our pipeline, a synthetic background image is created for each raw image using several images taken close in time to the original image. The synthetic background image is repeatedly refined to smooth it and to account for stars and other objects in the frame. We expect hundreds, if not thousands of images will need to be combined for each satellite image. The data reduction system architecture is shown in Fig. 8, and consists of a parallel blade or server architecture with Ethernet connections between the nodes. The algorithm is CPU-intensive and not dominated by storage or communications concerns.

8. Conclusion

HANDS-IONS is a system designed to track, characterize, and find geosynchronous, earth-orbiting satellites during the daytime using advanced infrared imaging technology. The camera is designed to work both during the day and night, and should have sufficient sensitivity to detect a large fraction of the GEO population. A summary of the capabilities of the camera is shown in Table 2.

Table 2: Technical specifications of the HANDS-IONS camera system

Location: Mauna Kea, Hawaii at the University of Hawaii 88-inch Observatory
Altitude: 4200 m

Telescope: Ritchey-Chretien telescope with 2.2-m primary, f/10 secondary, with fold mirror at bent-Cassegrain position (three mirror reflections to camera). All mirrors are aluminum-coated. Telescope mount: open yoke equatorial mount with a classical slit dome. Other telescopes upon which the camera is designed to mount readily: Air Force 1.6-m (Haleakala, HI), Mt. Lemmon Observing Facility (1.5-m) (Mt. Lemmon, AZ), and the W.L. Eccles 0.8-m (Frisco Peak, UT)

Camera: HgCdTe focal plane at cryogenic temperatures with refractive re-imaging optics and a Lyot stop for thermal masking. Helium-cooled with a remote compressor, optionally cooled instead with a Stirling-cycle cooler with glycol heat transport from cooler.

- Effective system focal length = 10.3 m
- system aperture = 2.2 m
- system f-number = f/4.68
- pixel scale = 0.4 arcsec/pixel
- timing accuracy = 10 μs (1 σ)

Filters: Two five-position filter wheels:

- FW 1: Lyot stops for different telescopes, wire-grid array for polarization imaging
- FW 2: J,H,K-short,K, cold blank (for darks)

Imaging Array: Raytheon Vision Systems MANTIS SB-339 HgCdTe focal plane array with 2.5 μm cut-off

- 1280 x 1024 pixels, 20 microns square
- 60 frames per second readout capable (currently limited to 20 fps by controller)
- full well is either 70Ke- w/25 e- read noise (CDS) or 2.5 Me- w/ 175 e- (single sample)
- non-destructive readout for 70 Ke- full well, capable of Fowler sampling
- global snap-shot shutter for 70 K e- full well

Operations:

- operating humidity: less than 90% relative humidity, non-condensing
- sun angle: no closer than 30° to the sun
- interfaced to infrared and optical all-sky cameras and weather systems
- interactive and scheduled observing programs
- near-real-time data reduction using on-site parallel computing cluster

Data products:

- satellite and star images
- photometric measurements of satellites and stars
- astrometric positions of satellites
- orbital ephemerides of satellites

This work is sponsored by the Advanced Technology Branch of the Space and Missile Systems Center (AFSPC SMC/SYE) under contract FA8819-10-C-0002, High Accuracy Network Determination System - Intelligent Optical Networks for Space Situational Awareness (HANDS-IONS), with Program Manager Capt. Eric Charest. The authors gratefully acknowledge the insight and advice of of Dr. Donald Davies and Dr. Ray Russell of the Aerospace Corporation and of Dr. Earl Spillar of AFRL.

9. References

1 Chesser, D.E., Vunck, D., Born, T., Axelson, W., Rehder, K., Medrano, R., NIR Daylight Acquisition Sensor Improves Mission Capabilities, *Acquisition, Tracking, and Pointing XVII*. Edited by Masten, Michael K.; Stockum, Larry A. Proceedings of the SPIE, Volume 5082, pp. 1-12 (2003).

2 Hall, D., Separating Attitude and Shape Effects for Non-resolved Objects, *Proceedings of the Advanced Maui Optical and Space Surveillance Technologies Conference*, held in Wailea, Maui, Hawaii, September 12-15, 2007, Ed.: S. Ryan, The Maui Economic Development Board., p.E51

3 Doyle Hall, personal communication.

4 Jim, K., Scott, B., Knox, R., Simulations of Non-resolved, Infrared Imaging of Satellites, *Proceedings of the* Advanced Maui Optical and Space Surveillance Technologies Conference, held in Wailea, Maui, Hawaii, September 1-4, 2009, Ed.: S. Ryan, The Maui Economic Development Board., p.E75

5 Jim, K., Rayner, J., Tokunaga, A., Pier, E., Gibson, B., Daytime Near-Infrared Astronomical Observing, in preparation.

6 Jim, K., Gibson, B., Pier, E., Proceedings of the Advanced Maui Optical and Space Surveillance Technologies Conference, held in Wailea, Maui, Hawaii, September 2011, in preparation.

7 Tokunaga, A.T., Simons, D.A., Vacca, W.D., The Mauna Kea Observatories Near-Infrared Filter Set. II. Specifications for a New JHKL'M' Filter Set for Infrared Astronomy, *The Publications of the Astronomical Society of the Pacific*, Volume 114, Issue 792, pp. 180-186

8 Raytheon Vision Systems, *SB339 –User's Manual*, November 19, 2010.

9 Corrales, E., Raytheon Vision Systems, private communications, 2011.

10 Onaka, P., Tonry, J., Isani, S., Lee, A., Uyeshiro, R., Rae, C., Robertson, L., Ching, G., Pan-STARRS PS1 STARGRASP Controller, The Advanced Maui Optical and Space Surveillance Technologies Conference, held in Wailea, Maui, Hawaii, September 10-14, 2006, Ed.: S. Ryan, The Maui Economic Development Board, p.E49

11 Tonry, J.L., Burke, B.E., Isani, S., Onaka, P., Cooper, M.J., Results from the Pan-STARRS Orthogonal Transfer Array (OTA), *Proceedings of the Society of Photo-Optical Instrumentation Engineers (SPIE) Conference Series*, Vol. 7021, pp. 702105-702105-9 (2008).